Proceedings of the
FOURTH INTERNATIONAL
KIMBERLITE
CONFERENCE
Perth 1986

Kimberlites And Related Rocks
Volume 1

THEIR COMPOSITION, OCCURRENCE,
ORIGIN AND EMPLACEMENT

PUBLISHED FOR THE GEOLOGICAL SOCIETY OF AUSTRALIA INC
BY BLACKWELL SCIENTIFIC PUBLICATIONS

GSA SPECIAL PUBLICATION NO. 14

7 Stability of amphibole and phlogopite in metasomatized peridotite under water-saturated and water-undersaturated conditions

K. MENGEL* and D. H. GREEN

Department of Geology, University of Tasmania, Hobart, Tasmania, Australia
**Present address: Geochemisches Institut, Universität Göttingen, Goldschmidtstr. 1, D-3400 Göttingen, FRG.*

ABSTRACT

High pressure experiments were carried out on a model metasomatized peridotite composition from the Northern Hessian Depression (NHD-peridotite) at water-saturated (plus 0.4% water) and water-undersaturated (plus 0.15% water) conditions. This peridotite represents a suitable source for the alkali-basalts from this region. It consists of a depleted (anhydrous peridotite xenoliths) and a metasomatic component (magnesian phlogopite from metasomatized xenoliths). At both water-saturated and water-undersaturated conditions, amphibole is stable up to 28 kb. Amphibole and phlogopite occur in a (small) temperature interval above the solidus at water-saturated conditions up to 25 kb. At lower water contents, the solidus of NHD-peridotite is determined by the stability of amphibole which breaks down above 1150°C at 25 kb and above 1050°C at 28 kb. Phlogopite is stable above the solidus to temperatures of 1175°C at 25 kb and to 1200°C at 30 kb. In the phlogopite-present as well as in the phlogopite-absent melting range, liquids coexist with ol, opx, cpx, (sp), and gar at pressures above 25 kb. The composition of these liquids could not be determined directly.

In an attempt to characterize the nature of these liquids, sandwich-experiments were carried out in which a basanite layer (glass plus 4% water) was embedded between two layers of NHD-peridotite presaturated with water. The compositions of the melts formed in the basanite layers at 28 kb 1250°C and at 28 kb, 1195°C were evaluated by mass balance from microprobe area scan analyses, the composition of the residual phases and the composition of the bulk charge. Liquids from both experiments are clearly basanitic to nephelinitic in composition. At 28 kb 1195°C, the Na/K ratio of the preferred liquid composition is close to that of subsolidus amphiboles at water-undersaturated conditions and to that of the input basanite. The melt formed at 28 kb, 1250°C has a Na/K ratio which is distinctly different from that of the input basanite. It is concluded that, for this model peridotite composition, the breakdown of amphibole is the key process which leads to the formation of basanitic melts like those from the Northern Hessian Depression and that the contribution of phlogopite plays a subordinate role.

Keywords: phlogopite, pargasite, peridotite solidus, mantle metasomatism, olivine nephelinite and basanite.

7.1 INTRODUCTION

Numerous geochemical models published over the past two decades suggest a metasomatic enrichment of the source peridotites for alkali basalts highly enriched in incompatible elements. Evidence for metasomatic alteration of depleted peridotite also arises from peridotite xenoliths brought to the surface by basaltic and kimberlitic magmas (e.g. Menzies & Murthy 1980; Mengel *et al* 1984; Dawson 1980). Amphibole and phlogopite are among the most important products of metasomatic reactions. Large proportions of the incompatible trace element content of the bulk peridotite are concentrated in these minerals. It is therefore necessary to study the stability of

these minerals in metasomatized peridotite compositions in order to examine their role in partial melting processes.

A number of previous experimental studies on natural peridotites have dealt with either amphibole stability (Kushiro *et al* 1968; Green 1973, 1976; Millhollen *et al* 1974; Mysen & Boettcher 1975) or with phlogopite stability (Wendlandt & Eggler 1980).

In this study, we have investigated the stability of amphibole and phlogopite in a natural metasomatized peridotite composition under water-saturated (peridotite plus 0.4% H_2O) and under water-undersaturated conditions (peridotite plus 0.15% H_2O). All phases in the run products, with the exception of glass, were analysed by electron microprobe as long as they were large enough (> 5μ).

7.2 EXPERIMENTAL METHODS

7.2.1 Starting material

The peridotite investigated is a model composition derived from extensive chemical investigations on depleted and metasomatized peridotite xenoliths (Mengel 1981; Oehm *et al* 1983; Hartmann & Wedepohl 1984; Wedepohl 1985) occurring in alkali basalts from the Northern Hessian Depression volcanic area of north-west Germany (NHD-peridotite). This composition was favoured by Wedepohl (1985) as a source for alkali-olivine basalts, basanites and nephelinites from this region. NHD-peridotite consists of a depleted and a metasomatic component. The depleted component (Table 7.1, column A) equals the average composition of 28 lherzolite and harzburgite xenoliths from this area and is very close in its major element composition to average depleted peridotite from worldwide sampling (Oehm *et al* 1983); its normative mineralogy is 73% olivine (ol), 18% orthopyroxene (opx), 7% clinopyroxene (cpx) and 1% Cr-spinel (sp). To this peridotite, an equivalent of 1.5% phlogopite (Table 7.1, column B) was added which represents the metasomatic component. The material investigated in experiments represents a composition of NHD-peridotite minus 60% olivine (Table 7.1, column C). Ol has been subtracted in order to diminish the dominance of this mineral and to facilitate the identification and microprobe analysis of minor phases. Sufficient quantities of olivine (> 25%) were still present in all experiments.

The starting mix was prepared from analytical grade reagents. In a first step, all components except ferrous iron were carefully ground under acetone and sintered at 1000°C. To this material ferrous iron was added as $FeSiO_4$ and this final mix was fired at 1000°C in an Ar-atmosphere.

For runs at water-saturated conditions, 1% water was added by a microsyringe to 14 mg of the starting mix. This equals 0.4% H_2O in the original NHD-peridotite (no ol subtracted). During sealing of the capsule, its base was kept at temperatures below 0°C. The capsule weight was checked before and after sealing, and after the experiments.

For runs at water-undersaturated conditions, 90–100 mg of the starting mix was presaturated with 2% water in large-capacity runs at 15 kb, 925°C for 48 h in $Ag_{75}Pd_{25}$. This approach was used to overcome unavoidable errors in pipetting very small amounts of water (≤ 0.05 mg). After the run, the capsule was pierced and dried out at 110°C. The run product was then ground under acetone and dried at 450°C. The amount of water remaining in the large-capacity-run products is 0.35–0.4 wt% H_2O which is equivalent to 0.15% H_2O in the original NHD-peridotite (no ol subtracted). This water is exclusively fixed in amphibole and phlogopite structures. The run product consists of a fine-grained assemblage of ol, opx, cpx, amph, phlog, and sp. Microprobe analyses of the constituent phases were used in a least-squares program to calculate their proportions. From this presaturated material, 10–12 mg were used in experiments under various P,T conditions.

TABLE 7.1 Chemical composition of the starting material.

	A	B	C*	D
SiO_2	43.4	40.52	47.20	43.79
TiO_2	0.08	1.06	0.25	2.75
Al_2O_3	2.0	17.92	5.60	12.19
Cr_2O_3	0.42	1.17	1.08	0.06
Fe_2O_3				3.63
FeO	8.6	5.42	6.69	7.58
MnO	0.13	0.03	0.07	0.17
MgO	43.1	23.35	33.59	11.87
CaO	1.8	0.09	4.43	11.62
Na_2O	0.13	0.95	0.35	3.50
K_2O	0.03	9.28	0.43	1.88
NiO	0.30	0.21	0.30	0.04
P_2O_5				0.90
Mg-#	89.9	88.5	89.9	73.6

Notes: A Depleted peridotite : average of 28 spinel peridotite xenoliths (NHD, Oehm *et al* 1983).
B Phlogopite from metasomatized lherzolite xenoliths from the same area (Mengel 1981).
C NHD-peridotite: (0.985 A plus 0.015 B) minus 60% olivine $_{Fo89.9}$
D NHD-basanite (Wedepohl 1985).
* Calculated modal mineralogy of the starting mix for water-undersaturated experiments (NHD-peridotite minus 60% olivine plus 0.4% H_2O): 30% olivine; 35% orthopyroxene; 8% clinopyroxene; 19% amphibole; 5% phlogopite; 1.5% spinel.

For use in sandwich-type experiments, a mix with the composition of NHD-basanite (Table 7.1, column D) was prepared in the same way as described for NHD-peridotite. From this mix, a glass with 4% water was prepared in a large capacity run at 5 kb, 1200°C. The glass composition was checked by microprobe and was found to be identical to column D, Table 7.1 within the analytical uncertainties.

7.2.2 Experimental procedure

All runs were carried out in a piston-cylinder high-pressure apparatus. Nominal pressures were maintained at ± 0.2 kb. Temperatures were measured with $Pt_{100}/Pt_{90}Rh_{10}$ thermocouples and automatically controlled to ± 6°C. A 13 mm diameter furnace assembly was used with NaCl or NaCl-Pyrex glass sleeves and Boron nitride spacers. For temperatures below 1175°C, $Ag_{75}Pd_{25}$ capsules were used and $Ag_{50}Pd_{50}$ capsules for runs at higher temperatures.

Iron loss which can be easily detected by zoned ol and pyroxenes and by unreasonably high 100Mg/Mg + Fe numbers ($Mg^{\#}$) was not observed in experiments at subsolidus conditions. In above-solidus runs with larger amounts of melt present, e.g. at 28 kb, 1250°C, severe iron loss was observed at a run duration of 48 h. At run times of 28 and 14 h, this effect became much smaller relative to the 48 h run. At run times of less than 10 h, no detectable iron loss occurred. Thus, run times of all above-solidus runs were confined to 8 h or less.

For experiments under water-saturated conditions including the large-capacity runs, there is evidence of small amounts of ferric iron in sp and cpx (and gar). The ferric iron content of the large-capacity run products is 0.5% Fe_2O_3 (Table 7.2), estimated on the base of the proportions of phases and the ferric iron content in cpx, opx and sp as calculated from microprobe analyses.

For sandwich-type experiments, a layer of NHD-basanite glass was packed between two layers of NHD-peridotite presaturated with water. The proportions peridotite/basanite were equal to 86/14. All other experimental details were the same as those for water-undersaturated experiments. The run time was confined to 1h to avoid iron loss. Homogeneity of phases throughout the charge (i.e. within the basanite layer and within the NHD-peridotite layers) suggests that equilibrium assemblages were obtained.

7.2.3 Phase identification, electron microprobe analysis

Experimental charges were recovered as sets of small discs. A small part of each charge was crushed and examined in refractive index oil. Above-solidus runs are detected by the presence of glass and quench outgrowths on grain surfaces. Runs at water-saturated conditions exhibit additional quenched vapour phase solutes which consists mainly of tiny amphibole and of phlogopite platelets.

Most experiments were analysed at the University of Tasmania with a JEOL electron microprobe fitted with an energy dispersive system. A smaller number of experiments was analysed with a wavelength-dispersive ARL-SEMQ II microprobe at the Geochemisches Institut of the University of Göttingen (FRG). In order to allow comparison of analytical results one biotite and one clinopyroxene standard were analysed with both instruments. The differences in concentrations of the major elements were within the statistical uncertainties of both instruments which are ± 1–5 % (relative).

Quench phases are distinguished from primary phases by their composition, e.g. quench amphibole and phlogopite have significantly lower Mg-#, higher Fe and Ti and lower Cr concentrations. Many subsolidus runs were very fine-grained and microprobe analysis of clinopyroxene, amphibole and spinel was often in error because of simultaneous excitation of nearby crystals.

Structural formulae of analysed phases were calculated from microprobe analyses on the basis of a fixed number of cations per formula unit. The ferric iron content of cpx, opx, sp, and gar was calculated from charge balance assuming a fixed number of oxygen atoms per formula unit. Ferric iron contents of amphibole and phlogopite were not calculated. Analyses of these phases given in Table 7.2, 7.3 and 7.4 are recalculated water-free.

TABLE 7.2 Composition of phases in experiments on NHD-peridotite minus 60% olivine. *Mg-#* : 100 Mg/Mg + Fe^{2+}.

Water-saturated conditions; 25 kb								
T	975°C				1000°C			
	amph	phlog	cpx	gar	amph	phlog	cpx	gar
SiO_2	45.29	39.21	51.67	41.74	46.20	42.13	52.18	41.90
TiO_2	0.82	1.06	0.44	0.46	0.96	1.28	0.36	0.96
Al_2O_3	14.14	19.21	4.51	21.15	12.02	16.20	3.94	21.34
Cr_2O_3	1.05	1.47	0.43	1.37	1.78	1.35	1.11	2.18
FeO	3.72	4.21	3.46	8.16	3.73	3.76	2.85	7.73
MgO	19.81	24.99	17.19	19.60	20.73	25.37	17.16	19.08
CaO	11.83	0.28	21.85	7.32	11.28	0.08	20.54	7.31
Na_2O	1.86	0.53	0.45	—	2.14	0.62	0.77	—
K_2O	1.48	9.04	—	—	1.46	9.22	—	—
Mg-#	90.4	91.4	89.9	81.0	90.7	92.3	91.7	81.5
Mg-#			95.5	85.3			93.5	82.6

Water-undersaturated conditions : 25 kb								
T	1150°C				1175°C		1200°C	
	amph	phlog	cpx	gar	phlog	cpx	gar	cpx
SiO_2	44.71	41.68	51.67	42.25	42.12	51.27	43.64	51.46
TiO_2	1.21	1.52	0.33	0.54	1.23	0.36	0.57	0.28
Al_2O_3	15.06	16.92	4.75	20.87	16.48	5.33	19.93	6.28
Cr_2O_3	1.72	1.28	0.97	2.53	0.76	0.93	1.47	1.28
FeO	3.88	3.79	2.79	6.51	3.26	2.90	6.81	3.19
MgO	18.95	24.87	17.41	19.88	25.99	17.90	21.19	18.47
CaO	11.49	0.23	21.43	7.32	0.00	21.11	6.39	18.36
Na_2O	1.77	0.34	0.46	—	0.28	0.50	—	0.68
K_2O	1.22	9.34	—	—	9.88	—	—	—
Mg-#	89.7	92.1	91.3	84.5	93.4	91.6	84.7	91.2
Mg-#			95.5	84.9			97.3	84.9

TABLE 7.3 Composition of phases in experiments on NHD-peridotite minus 60% olivine, water-undersaturated conditions *Mg-#* : 100 Mg/Mg + Fe^{2+}.

	28 kb						
T	1050°C				1100°C		
	amph	phlog	cpx	gar	phlog	cpx	gar
SiO_2	45.93	41.90	52.42	41.67	41.97	52.26	41.58
TiO_2	0.96	1.17	0.37	0.64	1.31	0.31	0.46
Al_2O_3	12.73	16.58	3.98	20.31	16.10	4.57	20.30
Cr_2O_3	1.24	1.41	1.69	2.61	1.75	1.26	3.24
FeO	3.95	3.68	3.24	7.57	3.73	2.79	7.22
MgO	19.98	25.41	16.96	19.81	25.09	17.85	20.37
CaO	11.07	0.05	20.99	7.40	0.00	20.19	6.84
Na_2O	2.47	0.49	0.96	—	0.58	0.77	—
K_2O	1.67	9.50	—	—	9.48	—	—
Mg^2	90.0	92.4	90.3	82.3	92.3	91.9	83.4
Mg^2			95.4	86.3		95.5	87.7

	28 kb						
T	1175°C		1200°C			1250°C	
	phlog	cpx	gar	cpx	gar	cpx	gar
SiO_2	41.39	51.47	41.17	51.85	41.68	51.18	42.05
TiO_2	1.12	0.28	0.53	0.22	0.28	0.28	0.33
Al_2O_3	16.48	5.4	21.74	5.65	20.74	6.09	21.61
Cr_2O_3	1.08	0.96	1.51	1.18	3.18	1.04	1.86
FeO	4.48	3.44	7.32	3.87	6.63	3.77	6.28
MgO	25.78	17.95	20.07	18.15	20.60	18.00	21.23
CaO	0.58	19.85	7.64	18.23	6.89	18.95	6.63
Na_2O	0.00	0.65	—	0.85	—	0.69	—
K_2O	9.09	—	—	—	—	—	—
Mg-#	91.1	90.3	83.0	89.3	84.7	89.5	85.8
Mg-#		95.9	89.5	92.7	89.0	94.4	89.0

7.3 EXPERIMENTAL RESULTS

The phase assemblages of experimental runs on NHD-peridotite are summarized in Figs. 7.1 A and B for water-saturated and water-undersaturated conditions, respectively.

7.3.1 Water-saturated conditions

The solidus was easily determined by the presence of quenched liquid and by textural changes in the run products, i.e. larger grain size of ol, opx, cpx (and gar). The solidus of NHD-peridotite minus 60% ol agrees closely with the water-saturated solidi of pyrolite minus 40% ol (Green 1973, 1976), St Paul's peridotite (Milhollen *et al* 1974) and a spinel lherzolite from Hawaii (Kushiro *et al* 1968). At 28 kb, amphibole becomes unstable between 900 and 950°C. The high pressure stability limit of amphibole in NHD-peridotite (Fig. 7.1A) is similar to that suggested by Milhollen *et al* (1974) for St Paul's peridotite and intersects the solidus at 2–4 kb lower pressure than the amphibole-breakdown curve for pyrolite (Green 1973). The sharp back-bending of the stability limit of amphibole in water-saturated peridotite at pressures as low as 20–24 kb (Mysen & Boettcher 1975; Olarssen & Eggler 1983) is not supported by these results.

Amphibole and phlogopite are stable above the solidus at 15–25 kb and phlogopite was observed above the solidus at 30 kb, 1035°C. These phases coexist with ol, opx, cpx, sp, (gar), and a liquid. Similar observations were made by Green (1973) and Millhollen *et al* (1974). Their studies suggest that amphibole coexists with a liquid in a small temperature interval of 30°C above the solidus at pressures ≤ 25 kb.

7.3.2 Water-undersaturated conditions

The solidus for NHD-peridotite minus 60% ol plus 0.4 wt% water coincides with the curve marking the disappearance of amphibole (Fig. 7.1B). Within the experimental brackets, amphibole does not appear above the solidus. Phlogopite, however, persists about 30°C above the solidus at 20 kb and more than 150°C above the solidus at 30 kb. The back-bending of the amphibole stability boundary between 25 and 28 kb leads to a wide field at higher pressures and T > 1000°C where small amounts of liquid coexist with residual ol, opx, cpx, phlogopite, sp, and gar. The amount of liquid present increases above phlogopite breakdown and would increase more rapidly as the anhydrous solidus is exceeded. The shapes of the solidus and the amphibole breakdown curve in NHD-peridotite at water-undersaturated conditions resemble those in pyrolite + 0.2% H_2O (Green 1973).

The linear shape of the high temperature stability of phlogopite in NHD-peridotite is similar to that suggested by Wendlandt and Eggler (1980) for a natural peridotite containing 10% additional phlogopite. However, in the range of 15–30 kb, their 'phlogopite-out' reaction curve lies at 30–50°C lower temperatures relative to NHD-peridotite. Quench phlogopite occurs at 25 kb, 1200°C and at 28 kb, 1250°C as relatively large platelets which cannot be distinguished from primary phlogopite at lower temperatures by optical inspection. A clear distinction is possible only by means of microprobe analyses. Comparison of the composition of quench and primary phlogopites reveals much higher Si, Ti, and Fe

TABLE 7.4 Composition of phases in 28 kb, 1195°C and in 28 kb, 1250°C experiments.

28 kb; 1195°C

	cpx		gar		phlog		melt	
	A	B	A	B	A	B	B	
SiO_2	51.85	51.39	41.68	42.08	42.08	41.39	45.4	CIPW
TiO_2	0.22	0.25	0.28	0.73	1.12	1.32	2.0	or 5.0
Al_2O_3	5.65	6.34	20.74	19.48	16.48	16.05	12.7	ab —
Cr_2O_3	1.18	1.42	3.18	3.07	1.08	1.82	—	an 20.5
FeO	3.87	3.19	6.63	6.65	4.48	3.25	7.9	lc 3.5
MgO	18.15	18.33	20.60	20.96	25.78	24.98	14.8	ne 9.7
CaO	18.23	18.15	6.89	7.03	0.58	0.00	12.7	di 33.7
Na_2O	0.85	0.87	—	—	0.00	0.22	2.1	ol 22.8
K_2O	—	—	—	—	9.09	10.23	1.6	il 3.9
Mg-#	89.3	91.1	84.7	84.9	91.1	93.2	77.0	
						FeO (K_D)	7.6	

28 kb; 1250°C

	cpx		gar		sp		melt	
	A	B	A	B	A	B		
SiO_2	51.18	51.49	42.05	41.73	—	—	46.2	CIPW
TiO_2	0.28	0.28	0.33	0.55	0.54	1.00	2.2	or 8.9
Al_2O_3	6.09	9.28	21.61	20.73	39.00	40.05	11.3	ab —
Cr_2O_3	1.04	0.77	1.86	3.08	21.79	25.80	—	an 13.6
FeO	3.77	3.44	6.28	6.58	19.68	14.03	7.7	lc 3.7
MgO	18.00	17.8	21.23	20.95	17.73	19.16	15.4	ne 10.6
CaO	18.95	18.42	6.63	6.93	—	—	11.5	di 34.7
Na_2O	0.69	0.70	—	—	—	—	2.3	ol 23.1
K_2O	—	—	—	—	—	—	2.3	il 4.2
Mg-#	89.5	90.6	85.5	85.3	61.6	70.9	78.0	
						FeO (K_D)	7.6	

Notes: A, non-sandwich-experiment; B, sandwich-experiment. FeO(K_D): calculated according to the Mg-Fe ol-liq K_D of Takahashi & Kushiro (1983).

and much lower Mg and Cr contents in the quench phlogopites.

In NHD-peridotite, garnet becomes a stable phase at pressures of 20 kb at 950°C, above 24 kb at 1150°C and above 25 kb at 1175°C. The amount of spinel present decreases greatly with the appearance of garnet.

7.4 COMPOSITION OF PHASES

Microprobe analyses of phases in some key experimental runs are given in Tables 7.2A and 7.2B. At water-saturated conditions, all phases including amphibole, phlogopite and clinopyroxene are quite similar in composition below and above the solidus at 25 kb and no systematic changes are observed in their Na/K ratios. Comparable experiments on pyrolite plus 6% water (Green 1976) also gave a rather constant Na/K ratio of amphiboles below and above the solidus at 15 kb. At both water-saturated and water-undersaturated conditions, the Na/K ratio of amphibole ranges between 1.5 and 2.2. It is different from the Na/K ratio of the starting composition (1.2) and the presence of coexisting phlogopite demonstrates effective potassium saturation of the pargasitic amphibole, i.e. Na/K ratios may be regarded as minimum values for pargasite at these P,T conditions.

Unlike in experiments on pyrolite (Green 1973), no marked increase in the 100Mg/Mg+Fe^{2+} ($Mg^{\#}$) of olivine, orthopyroxene and clinopyroxene are observed for NHD-peridotite when the solidus is crossed under water-saturated conditions. The increase in Mg-# of residual phases in water-saturated pyrolite experiments at 15 kb was explained by the presence of relatively

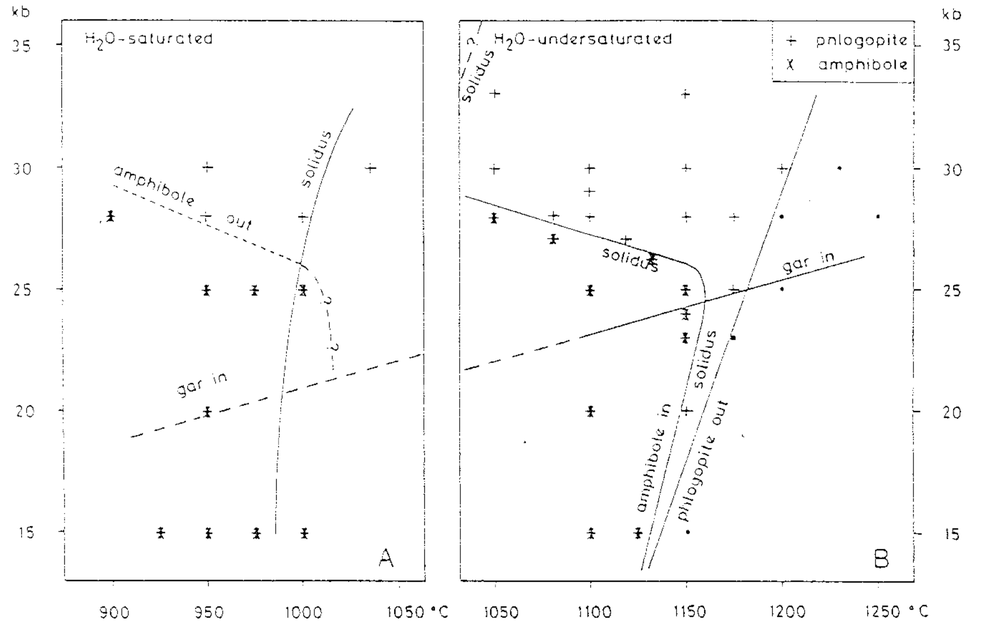

Fig. 7.1 Experimental determination of the solidus and the stability of amphibole and phlogopite in NHD-peridotite minus 60% ol at water-saturated (A) and water-understaturated (B) conditions. Phases coexisting with phlogopite (and amphibole) are ol, opx, cpx, sp, (and gar).

large melt fraction (Green 1976) and it is important that these experiments used 10% water in the charges. Because there is no such significant increase in Mg-# of the crystalline phases (Fig. 7.2A), the melt fractions present in NHD-peridotite at 25 kb at water-saturated conditions must be very small. This is consistent with the much smaller amount of water (1%) added to the charge. Thus, we believe that the degree of partial melting in the 25 kb, 1000°C experiment is in the order of a few percent.

In Fig. 7.2B, the *Mg-#* vs temperature relations in NHD-peridotite are summarized for water-undersaturated conditions at 25 and 28 kb. An increase in *Mg-#* for crystalline phases is observed at 25 and 28 kb when the solidus is crossed and further increase in *Mg-#* in olivine and orthopyroxene is observed at higher temperatures. Garnet and clinopyroxene show more complex changes which are not fully understood and may reflect in part the inclusion of Fe-rich quench outgrowths on clinopyroxene in the analyses. Coexisting garnet and clinopyroxene show the widest separation in *Mg-#* emphasizing their greater utility for geothermometry. The composition of clinopyroxene changes across the phlogopite breakdown curve with decreases in *Mg-#* and Ca/Al and increases in Na and Cr contents. These changes may reflect changes in liquid compositions (Table 7.4) and/or the problem of quench rims noted above.

7.5 SANDWICH EXPERIMENTS

In order to characterize the nature of the liquids in the phlogopite-present melting interval and in the phlogopite-absent melting region, peridotite-basanite sandwich experiments were carried out at 28 kb, 1195°C and at 28 kb, 1250°C. During the experiments, the basanite layer stayed in its position between the two peridotite layers. It consists of glass and variable but large amounts of quench-clinopyroxene (plus rare quench-apatite- and -phlogopite). The liquid composition could not be analysed directly by microprobe.

Even though there was no *a priori* information about the composition of the liquids, two import-

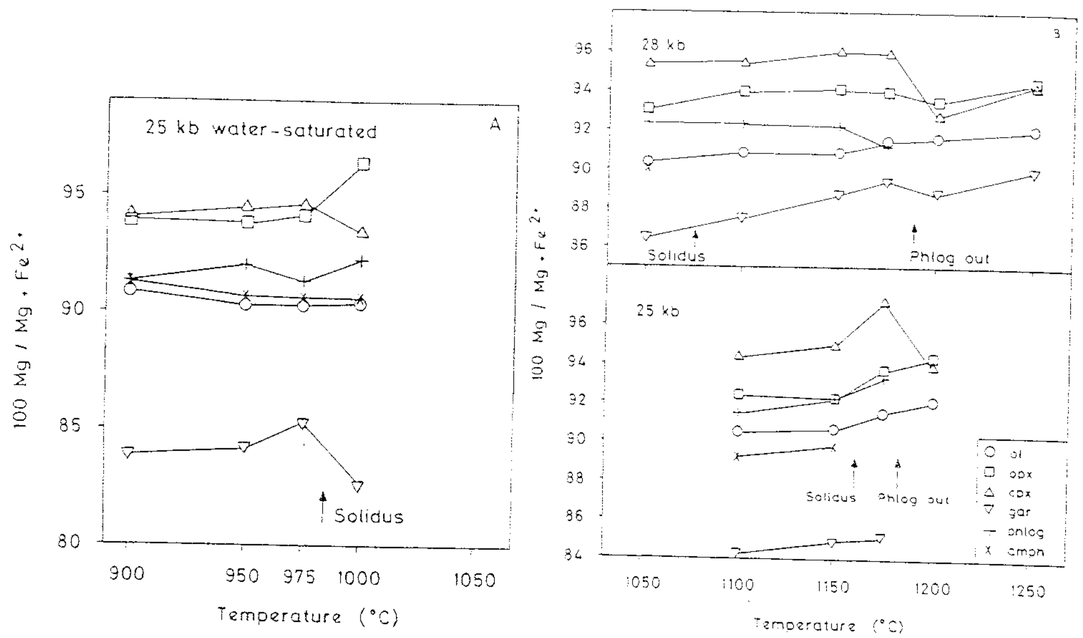

Fig. 7.2 Plot of temperature versus 100 Mg/Mg+Fe^{2+} for phases analysed in NHD-peridotite at water-saturated conditions, 25 kb (A) and at water-undersaturated conditions, 25 and 28 kb (B).

ant observations were made which indicate that these sandwich experiments were successful, i.e. that the compositions of the melts produced are close to the equilibrium partial melts of NHD-peridotite at 28 kb in phlogopite-present and phlogopite-absent conditions: (i) in both sandwich experiments, the residual phase assemblages were the same as in non-sandwich experiments at the same pressure and practically the same temperatures. With the exception of spinel and of the Cr and Ti concentrations in some other phases, there are no significant differences in the composition of the residual phases between the sandwich and the non-sandwich experiments (Table 7.4); (ii) small amounts of quenched liquid also occur within the peridotite layers. Microprobe analyses with a defocused beam gave up to 0.3 wt% P_2O_5 for such glass + quench patches. Because no P_2O_5 had been added to the starting material of the peridotite layers, this is taken as evidence for a sufficient mixing between the embedded basanite melt and the melt formed within the peridotite layers. This observation along with the good conformity of residual phases in the sandwich and the non-sandwich experiments indicates that the melts formed in both sandwich experiments are close to equilibrium melt compositions.

In order to determine the composition of the basanite layer small areas (5 × 5 to 50 × 50 µm) were analysed with a scanning electron beam so that different amounts of glass and quench-products were included. These scan analyses were plotted in a Mg-# versus oxides diagram over a large range of Mg-# (72–85) (Fig. 7.3A and B). Na was excluded from these plots because of vaporization problems. Within the data sets from both sandwich experiments, all major element oxides are correlated with the Mg-#, with the exception of Cr_2O_3 and of TiO_2 in the 28 kb, 1195°C run. From Mg-# – oxide regression lines, a set of hypothetical liquid compositions were calculated for Mg-# 72–80. These data were then used together with the composition of the residual phases and that of the bulk charge in least-squares calculations to evaluate the proportions of residual phases and liquid. For both sandwich experiments, we used SiO_2, TiO_2, Al_2O_3, FeO, MgO, CaO, and, in addition, K_2O for the 28 kb, 1195°C sandwich experiment. For each experiment, only one out of all hypothetical liquid compositions

(Mg-#72–80) gave a satisfactory solution which gave positive proportions for all residual phases. All other hypothetical liquid compositions gave negative results for at least one of the residual minerals. The liquid composition selected for the 28 kb, 1195°C is that with a Mg-# of 77 and for the 28 kb, 1250°C sandwich experiment, the equilibrium liquid composition is that at Mg-# 78. Calculated degrees of melting are 31% and 37% of the capsule contents, respectively. The compositions of these melts are given in Table 7.4 along with their CIPW-norms. The Na_2O concentrations were calculated from the relative proportions of melt and residual cpx and the Na_2O contents of the bulk charge and of cpx.

The liquids formed in both sandwich experiments are clearly basanitic, transitional to nephelinitic in the absence or normative albite and in the very high normative diopside contents. In comparison with the spectrum of mantle-derived liquids for the Northern Hessian Depression given by Wedepohl (1985) the analysed liquids from the experiments are close to the nepheline-rich basanite composition (Table 7.1). However, they have higher normative olivine, lower normative nepheline (+ albite) and ilmenite contents. Some differences in normative mineralogy reflect the unknown Fe_2O_3 content of the analysed liquids but other differences (higher SiO_2, higher MgO, lower Na_2O) are tentatively attributed to a failure to exactly match P,T conditions and source composition for the natural NHD nepheline basanites. It is possible that slightly higher pressures (30–35 kb) may have produced a better 'match' between experimental and natural magmas. The problem of quench crystallization and resulting analytical scatter (Fig. 7.3A, B) suggests that comparisons should not be pushed too closely, e.g. the *increase* in concentration of all of the incompatible elements Na_2O, K_2O and TiO_2 from 1195°C to 1250°C is unlikely, particularly as P_2O_5 content decreases.

However, we consider that our data demonstrate that liquids at 28 kb 1195°C to 1250°C in equilibrium with olivine, orthopyroxene, clinopyroxene and garnet (± spinel, ± phlogopite) are olivine- and nepheline-rich basanites transitional to olivine nephelinites. These liquids require the

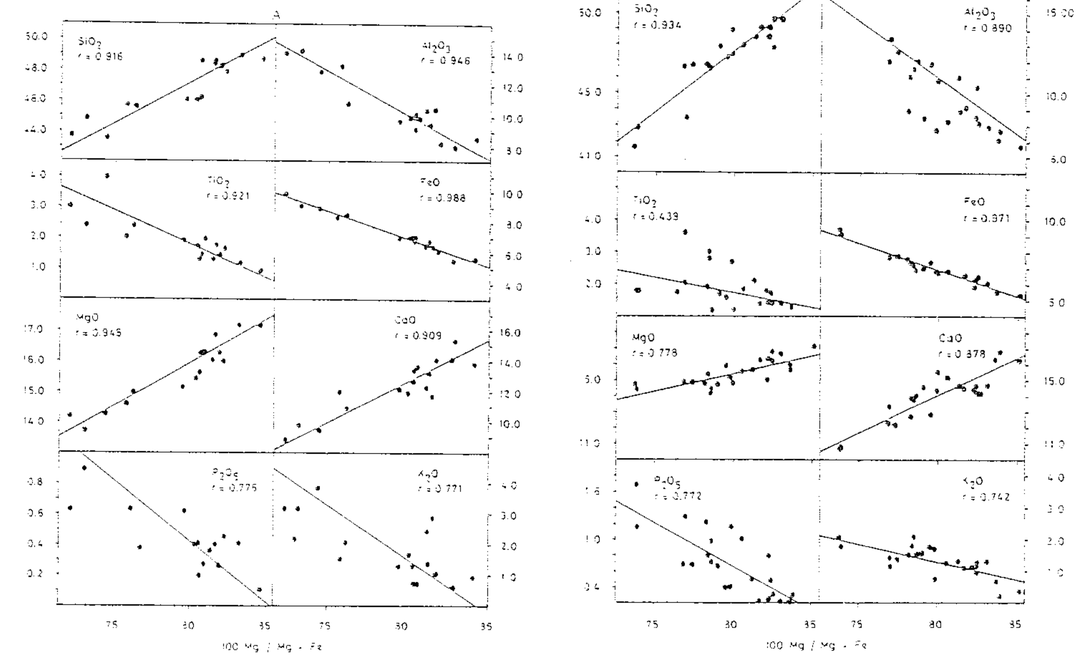

Fig. 7.3 Plot of major element oxides versus Mg-# of microprobe area scan analyses of the basanite layer in sandwich-experiments at 28 kb, 1250°C (A) and at 28 kb 1195°C (B).

presence of small amounts of water but do not require CO_2 ($CO_3^=$) in the source peridotite. Our data also demonstrate the surprising result that liquids of this highly undersaturated character developed in equilibrium with residual phlogopite have lower K_2O contents and higher Na/K ratios than the liquids formed immediately above phlogopite breakdown (Table 7.4). Basanitic liquids in which Na/K ≤ 1, appear likely to indicate temperatures of magma genesis marked by phlogopite instability. Referring to the analytical data set for the Northern Hessian Depression basalts (Wedepohl 1985), it is probable that all basanites to olivine melilite nephelinites with $K_2O \geq 1.6\%$ and MgO ≥ 10% were formed leaving residual phlogopite.

7.6 CONCLUSION

The majority of peridotite xenoliths in continental alkali-basalts consist of depleted spinel lherzolites and harzburgites which are free of amphibole and phlogopite, indicating that the subcontinental lithospere is largely anhydrous. The solidus of depleted, anhydrous peridotite is not intersected by any reasonable steady-state geotherm (< 150 mW/m^2). The introduction of small amounts of a metasomatic fluid which is rich in water, K, Al, and Ti leads to a decrease of the solidus temperature and to the formation of subsolidus amphibole and phlogopite. The solidus ('amphibole dehydration solidus') of such metasomatized peridotite has a characteristic shape (Green 1973, fig. 2). Subsequent diapirism and melting of this enriched mantle at P ~ 25–30 kb leads to the formation of basanitic melts over a large temperature range. The K/Na ratio and the K content of a melt which is saturated with phlogopite (e.g. at 28 kb, 1195°C) are lower than expected and are similar to K/Na ratios of undifferentiated basanites to nephelinites from the Northern Hessian Depression. Extraction of such liquids leads to a phlogopite bearing residuum with increased K/Ca and probably increased Rb/Sr ratios. Small and slightly varying amounts of phlogopite in a depleted peridotite can produce significant small scale and large scale $^{87}Sr/^{86}Sr$ heterogeneities in a few tens of million years and might be responsible for the range of $^{87}Sr/^{86}Sr$ initial ratios observed in regions with multistage volcanic activity.

ACKNOWLEDGMENTS

The authors are indebted to K.L. Harris for invaluable assistance in the experimental work. KM wishes to express his gratitude to the petrological group of the Geology Department of the University of Tasmania for many fruitful discussions. This study was sponsored by the Australian Research Grant Scheme and by the Deutsche Forschungsgemeinschaft (Bonn, FRG) which is also gratefully acknowledged. G. Mengel is thanked for help in the preparation of the draft manuscript.

REFERENCES

Dawson J.B. 1980. *Kimberlites and their xenoliths*, 252 pp. Springer, Berlin, Heidelberg, New York.

Green D.H. 1973. Experimental melting studies on a model upper mantle composition at high pressure under water-saturated and water-undersaturated conditions. *Earth Planet. Sci. Lett.* 19, 37–55.

Green D.H. 1976. Experimental testing of "equilibrium" partial melting of peridotite under water-saturated, high-pressure conditions. *Can. Mineralogist* 14, 225–268.

Hartmann G. & Wedepohl K.H. 1984. Ausgewählte Spurenelemente in Peridotit-Xenolithen mit unterschiedlicher metasomatischer überprägung. *Fortschritte der Mineralogie* 62 (1), 82–84.

Kushiro I., Syono Y. & Akimoto S. 1968. Melting of a peridotite nodule at high pressures and high water pressures. *J. Geophys. Res.* 73, 6023.

Mengel K. 1981. Petrographische und geochemische Untersuchungen an Tuffen des Habichtswaldes und seiner Umgebung und an deren Einschlüssen aus der tieferen Kruste und dem oberen Mantel. PhD Diss. Universität Göttingen (FRG).

Mengel K., Kramm U., Wedepohl K.H. & Gohn E. 1984. Sr isotopes in peridotite xenoliths and their alkali host rocks from the northern Hessian Depression. *Contrib. Mineral. Petrol.* 87, 369–375.

Menzies M. & Murthy V.R. 1980. Nd and Sr isotope geochemistry of hydrous mantle nodules and their host alkali basalts: implications for local heterogeneities in metasomatically veined mantle. *Earth Planet. Sci. Lett.* 46, 323–334.

Millhollen G.L., Irving A.J. & Wyllie P.J. 1974. Melting interval of peridotite with 5.6 per cent water to 30 kilobars. *J. Geol.* 82, 575–587.

Mysen B.O. & Boettcher A.L. 1975. Melting of a hydrous mantle: I. Phase relations of natural peridotite at high pressures and temperatures with controlled activities of water, carbon dioxide, and hydrogen. *J. Petrol.* 16, 620–548.

Oehm J., Schneider A. & Wedepohl K.H. 1983. Upper mantle rocks from the area of the northern Hessian Depression (NW-Germany). *Tschermaks Mineralogisch Petrographische Mitteilungen* 32, 25–48.

Olafssen M. & Eggler D.H. 1983. Phase relations in amphibole, amphibole-carbonate, and phlogopite-carbonate peridotite: petrological constraints on the asthenosphere. *Earth Planet. Sci. Lett.* 64, 305–315.

Takahashi E. & Kushiro I. 1983. Melting of a dry peridotite at high pressure and basalt magma genesis. *Am. Mineralogist* 68, 859–879.

Wedepohl K. H. 1985. Origin of Tertiary basaltic volcanism of the northern Hessian Depression. *Contrib. Mineral. Petrol.* 89, 122–143.

Wendlandt R.F. & Eggler D.H. 1980. The origin of potassic magma: 2. Stability of phlogopite in natural spinel lherzolite and in the system $KAlSiO_4$-MgO-SiO_2-H_2O-CO_2 at high pressures and high temperatures. *Am. J. Sci.* 280, 421–458.